Optimizing the Geometry of the Focusing Horn Magnets in the Long-Baseline Neutrino Experiment Beamline

Jacob Kiefer
Cornell University, Ithaca, New York, 14853

Mary Bishai
Brookhaven National Laboratory, Upton, New York, 11973

August 8, 2012

Abstract

We report the results of our simulations for electron neutrino appearance at the far detector in the proposed LBNE(Long Baseline Neutrino Experiment) experiment as a function of the geometry of the focusing horn magnets and cylindrical graphite target located one kilometer before the near detector. The current setup of the beamline is a target distance of 45cm, with horn current of .20 MA in both horns, and horn spacing of 6m. We used the horn shape of the existing NuMI(Neutrinos at the Main Injector) horns at Fermilab. The 0-15 GeV neutrino energy range optimal horn/target geometry and currents for maximum electron neutrino flux are: the target located 50cm before horn 1 in the beamline, spacing between the horns at 10m, and .30 MA current for both horns using the NuMI horns. For the more important neutrino energy range of 0-2 GeV where oscillations are more readily observable, however, the optimal horn/target geometry and currents are: the target located 0cm target before horn 1 in the beamline, horn spacing between horns at 6m, and .22 MA horn current for both NuMI horns. These optimizations provide a significant yield, increasing the current capabilities of the NuMI beamline

by 32.0% for 0-15 GeV and and 23.8% for the 0-2 GeV neutrino energy case. Additionally, there is an intersection of the two optimal regions at: the target 30-40cm before horn 1 with a horn current of .28-.30 MA, which gives an increase in yield of 18.9% over 0-15 GeV and 14.9% over 0-2 GeV. In the horn current optimization, the best currents are: .4 MA horn 1 and .5 MA horn 2 for 0-15 GeV and .25 MA in both horns for 0-2 GeV. The 0-15 GeV horn current optimization give a 53.8% increase, while the 0-2 GeV optimization gives a 13.2% increase in electron neutrino yield when compared to .20 MA in both horns.

1 Introduction

In the path forward for neutrino physics, there are still a few major pieces of information still missing; two of the most important bits being the hierarchy of the three neutrino masses, and a parameter that governs neutrino properties called the CP angle [1]. The discovery of this information would revolutionize not only neutrino physics as we know it, but also possibly how physicists view the entire universe. Indeed, neutrino physics could contain explanations for why there is a disparity in the amounts of matter and antimatter in the universe, among other perplexing puzzles modern physics faces [2].

In an effort to experimentally determine these very important characteristics of neutrinos, the LBNE has been proposed [4]. Because the proposed experiment is so large and costly, many preliminary simulations need to be run to determine the most optimal and technically feasible solutions to achieve the desired results. The basic premise behind neutrino production in the current NuMI beamline is as follows: a high intensity proton beam is accelerated to high energy and hits an 80cm long cylindrical graphite target with radius of 6mm, producing positively and negatively charged pions that spew out in all directions [3]. These pions are focused into a beam by the two focusing horn magnets, which are parabolic in shape and have large currents running through them [3]. Depending on the sign of the current through the horns, the focusing horn magnets bend the trajectory of the positive or negative pions so that they travel in the desired path toward a detector [3]. Positive pions decay into positive muons and muon neutrinos, and negative pions decay into negative muons and muon antineutrinos [1]. The LBNE beamline is

the next generation of the NuMI beamline, and plans to add optimizations to increase the neutrino events detected and to increase sensitivity to the unknown neutrino parameters [4]. In the LBNE, a long cylindrical decay pipe is added, in order to reduce the background and give the LBNE very good signal to background ratio and therefore high statistics [4]. As they are travelling through the decay pipe, the pions decay into neutrinos in the direction of their momentum vector [1]. These neutrinos then travel approximately 1300km before they hit a very large detector made of liquid argon buried in the Homestake Mine located in South Dakota [4].

2 Flavor Oscillation

One of the key characteristics about neutrinos is their apparent ability to oscillate between flavors. The three flavors of neutrinos that we know about so far are electron, muon, and tau neutrinos, each corresponding to a partner charged lepton in the standard model [1]. This oscillation is a result of each neutrino being a different superposition of three quantum mechanical mass eigenstates, each of which are only slightly different from each other. These mass differences cause the phases of the quantum mechanical mass states to propagate at a different rate, thus resulting in a changing mixture of the masses as the neutrino travels through space and therefore flavor oscillation [1].

There are two modes of neutrino propagation that are of interest in the LBNE: muon neutrino to electron neutrino oscillations, and muon neutrino to muon neutrino survival [4]. The neutrinos produced by the proton beam hitting the target are muon neutrinos and throughout their trajectory toward the far detector, there is a finite probability that these muon neutrinos will oscillate to electron neutrinos. By measuring the number of muon and electron neutrinos detected at the far detector, we can discern information both the CP violation of neutrinos as well as the hierarchy of the three masses [4]. The probabilities of each of the oscillation and survival modes occurring are given by the following equations:

$$P(\nu_\mu \to \nu_\mu) = 1 - \sin^2(2\theta_{23}) \sin^2(1.27\Delta m^2_{32} \frac{L}{E}) \tag{1}$$

$$P(\nu_\mu \to \nu_e) \cong \sin^2 2\theta_{13} T_1 - \alpha \sin 2\theta_{13} T_2 + \alpha \sin 2\theta_{13} T_3 + \alpha^2 T_4 \tag{2}$$

$$T_1 = \sin^2 \theta_{23} \frac{\sin^2[1-x]\Delta}{(1-x)^2} \tag{3}$$

$$T_2 = \sin\delta \sin 2\theta_{12} \sin 2\theta_{23} \sin\Delta \frac{\sin(x\Delta)}{x} \frac{\sin[(1-x)]\Delta}{(1-x)} \tag{4}$$

$$T_3 = \cos\delta \sin 2\theta_{12} \sin 2\theta_{23} \cos\Delta \frac{\sin(x\Delta)}{x} \frac{\sin[(1-x)]\Delta}{(1-x)} \tag{5}$$

$$T_4 = \cos^2 \theta_{23} \sin^2 \theta_{12} \cos\Delta \frac{\sin^2(x\Delta)}{x^2} \tag{6}$$

with $\alpha \equiv \Delta m^2_{21}/\Delta m^2_{31}$, $\Delta \equiv \Delta m^2_{31} L/4E$, and $x \equiv 2\sqrt{2} G_F N_e E/\Delta m^2_{31}$

where $\sin^2\theta_{ij}$ are the neutrino mixing parameters, $|\Delta m^2_{ij}| = |m^2_i - m^2_j|$ are the absolute values of the neutrino mass differences squared, L is the distance traveled by the neutrino, E is the neutrino's energy, and G_F is the Fermi coupling constant [1]. The mixing parameters and mass differences are known precisely. The values used for this simulation are:

parameter	value
$\sin^2 2\theta_{12}$	.869
$\sin^2 2\theta_{23}$	1.00
$\sin^2 2\theta_{13}$	.100
Δm^2_{21}	$+7.59\times10^{-5}$ eV^2
$\lvert\Delta m^2_{32}\rvert$	2.32×10^{-3} eV^2

Table 1: Values used for mixing parameters and mass differences for neutrinos [1].

with the length to the far detector as L= 1300km and the neutrino energy output by the simulator [4]. There are three major factors that affect the flavor oscillation probabilities: the value of δ_{cp}, the ordering of the masses, and whether the particle in question is a neutrino or an antineutrino [2]. The following plots show the variations of the probability curves with respect to these three variables.

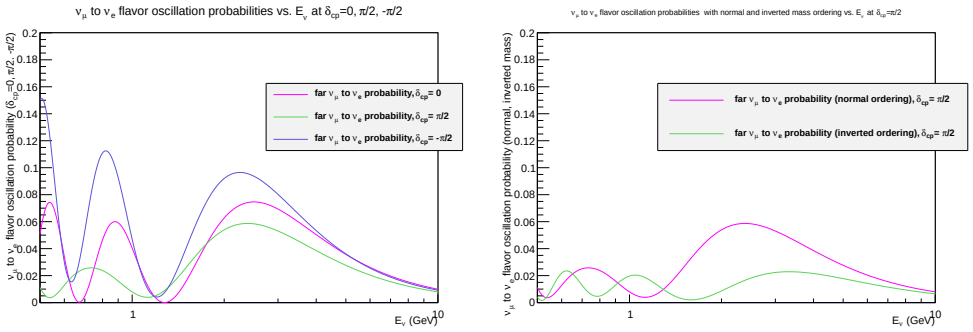

Figure 1: Neutrino flavor oscillation probability curves changing with respect to the δ_{cp} and the mass ordering.

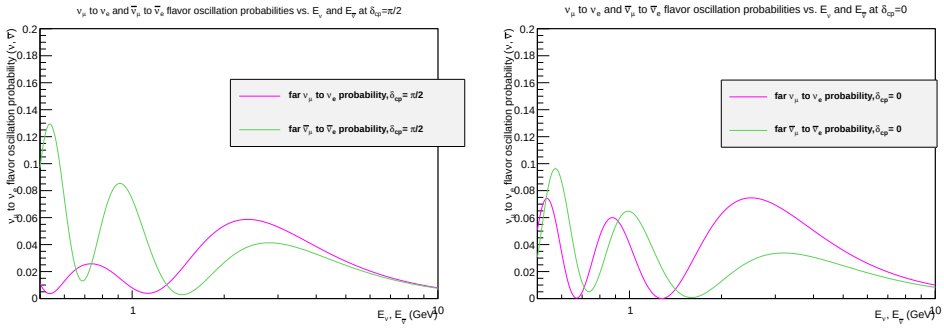

Figure 2: Neutrino flavor oscillation probability curves changing with respect to neutrinos/antineutrinos for two different values of δ_{cp}.

3 Experimental Setup and Procedure

With this general knowledge of neutrino physics, our task was to explore the effects of target position with respect to the horn, and horn current on the electron neutrino yield at the far detector using the GEANT4 LBNE simulator. GEANT4 is simply a large simulation package that was developed to simulate the passage of particles through matter [6] [7]. The parameter space for optimizing the horn geometry is complicated, since many factors determine how well the magnets can focus the pion beam [4]. The parameters that we varied to explore the neutrino yield were: target distance from horn 1, horn current (both holding the same and varying with respect to the other), and horn distances from one another as shown in Figure 3.

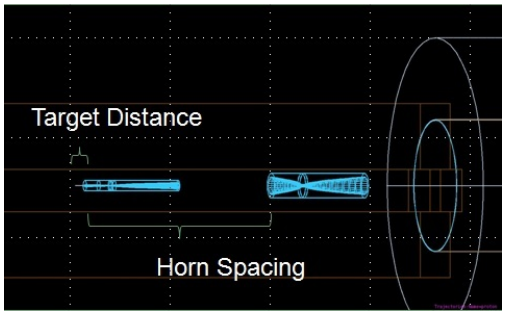

Figure 3: The conventions for measuring target distance and horn spacing.

Using a Monte Carlo procedure, we varied different parameters in the

input file to the GEANT4 simulator, ran the simulation of 2,500,000 protons for that specific target distance, horn currents, horn spacing, etc, and analyze the output files using a PyROOT interface [6] [7] [8]. To verify that the GEANT4 simulations were correct, we simulated the neutrino flux results for both the near and far detector from the MINOS experiment [3]. GEANT4 and PyROOT produced plots that were within 10-20% of the measure neutrino interaction rate in the MINOS near detector depending on the neutrino energies [3].

Though the focusing horn parameters were varied from simulation to simulation, the general projected experimental setup for LBNE remained the same for each simulation. Inasmuch, the total mass of the far detector was 10 kilotons, with detection efficiency of 80% for electron neutrinos and 85% for muon neutrinos, and fiducial mass considered to be 100% total mass [4]. The simulations also were scaled to 1×10^{21} protons on target [4]. The cross-section for neutrinos used was $.667 \times 10^{-42}$ m^2/GeV/nucleon$\times$neutrino energy [1].

With these experimental parameters and the varied horn geometry, the simulator would calculate the energy and parent particle weight for each neutrino, among other outputs. PyROOT would then plot a histogram of the distribution of neutrino events for each flavor over the energy spectrum of 0-15 GeV for that instance of the simulation [8]. In order to visualize the two flavors of neutrinos on the same histogram as shown in Figure 4, the electron neutrino distribution plot is multiplied by a factor of 10, which is noted in the legend of the plot. Additionally, since the value of the CP angle is unknown, the histogram is plotted for three values of the CP angle, $\delta_{cp} : 0, \pi/2, -\pi/2$.

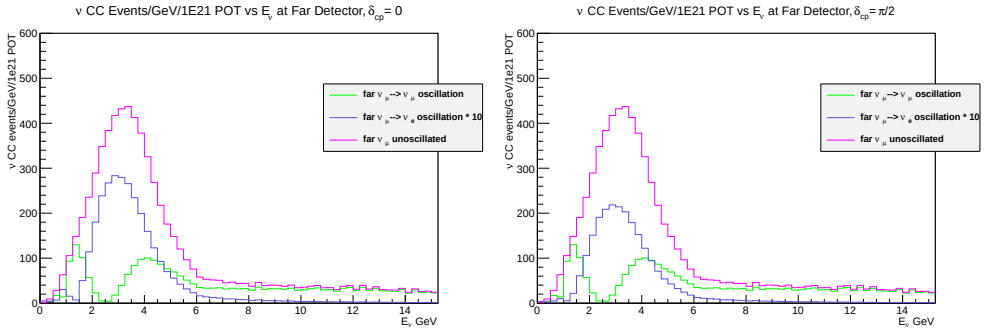

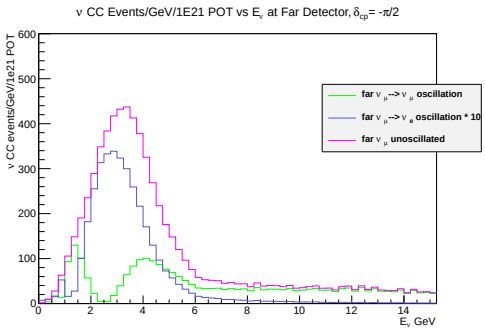

Figure 4: Neutrino event distributions over the 0-15 GeV energy spectrum for three values of δ_{cp} for 10cm target distance and .25 MA horn current at 6m horn spacing.

From these distribution plots, an integrated number of electron neutrino events as well as a χ^2 fit comparing $\delta_{cp} = 0, \pi/2$ (in terms of neutrino events, where $\delta_{cp} = 0$ is taken as expected value and $\delta_{cp} = \pi/2$ is observed, over 0-6 GeV) is taken for the whole energy spectrum as well as the interval from 0-2 GeV. The 0-2 GeV energy interval is the region where the effects of flavor oscillation are most apparent due to the larger differences in the probability curves as seen in Figures 1 and 2 [2]. The following equations were used to calculate the χ^2 fit:

$$\chi^2 = \sum_{k=1}^{n} (O_k - E_k)^2 / E_k \tag{7}$$

$$\tilde{\chi}^2 = \chi^2 / d \tag{8}$$

with O_k as the observed value, E_k as the expected value, $\tilde{\chi}^2$ as the reduced chi squared, and d as the degrees of freedom, or in our case the number of bins from 0-6 GeV: 24 [5].

After they are calculated, the integrated numbers of neutrino events and χ^2 values are then extracted for several iterations of simulations with various input parameters for the horn geometry and plotted against the geometric parameter that was varied in order to find maxima and then compared to the simulated values of the current LBNE beamline setup. The current LBNE

setup is a target distance of 45cm, .20 MA in both horns, and a horn spacing of 6m [4]. In maximizing the electron neutrino number, we ar trying to increase the amount of event data we receive from the LBNE. By maximizing χ^2, we are finding the regions of the phase space where we have the most sensitivity to variances in δ_{cp} [4]. The most important of these studies was optimizing the target distance in combination with the horn currents with the same current. These results are plotted below in Figure 5.

4 Results

The extracted results for varying the horn current versus the target distance upstream from horn 1 for both the 0-15 GeV energy spectrum and 0-2 GeV in terms of electron neutrino flux are shown below for $\delta_{cp} = 0$. The shapes of the contours do not change with δ_{cp}, so we can extract an optimal geometry from these plots even though the total integrated number of electron neutrinos varies. From Figure 5, we see that the optimal geometry and cur-

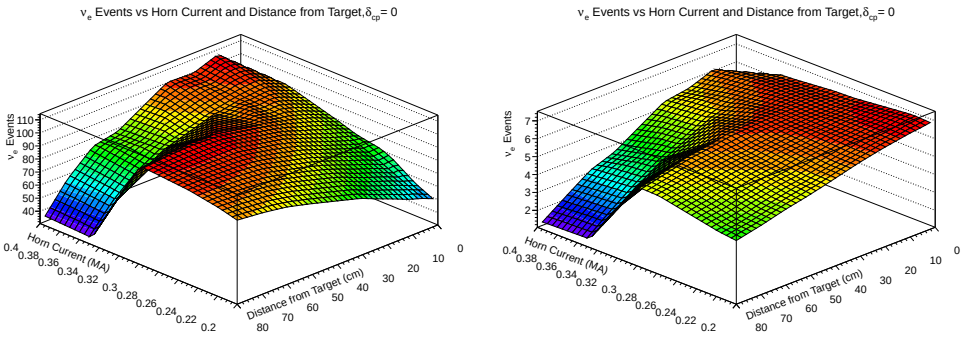

Figure 5: Electron Neutrino Events versus horn current and target distance over the 0-15 GeV interval and 0-2 GeV interval, respectively, with $\delta_{cp} = 0$. The horn spacing is fixed at 6m.

rents are: 50cm target distance and .30 MA horn current for 0-15 GeV and 0cm target distance and .22 MA horn current for 0-2 GeV. These optimizations give an electron neutrino yield increase of 32.0% and 23.8% respectively.

The extracted results for the χ^2 fit of the horn current versus target distance are shown in Figure 6, yielding a large region with high sensitivity to δ_{cp}.

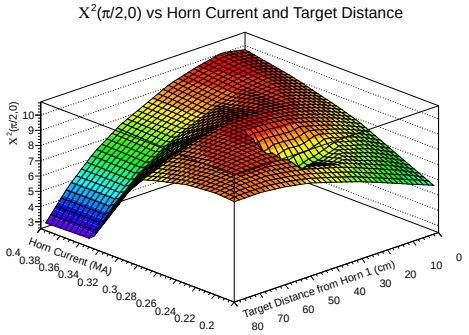

Figure 6: χ^2 fit comparing δ_{cp} =0, $\pi/2$ versus target distance and horn current. The horn spacing is fixed at 6m.

Another important variable that determines the neutrino flux at the far detector along with horn current and target distance is the horn spacing with respect to one another. The current setup of the LBNE beamline has the horn spacing at 6m. Figures 7 and 8 show the number of electron neutrinos as a function of horn spacing with the target at a distance of 10cm and 45cm, respectively.

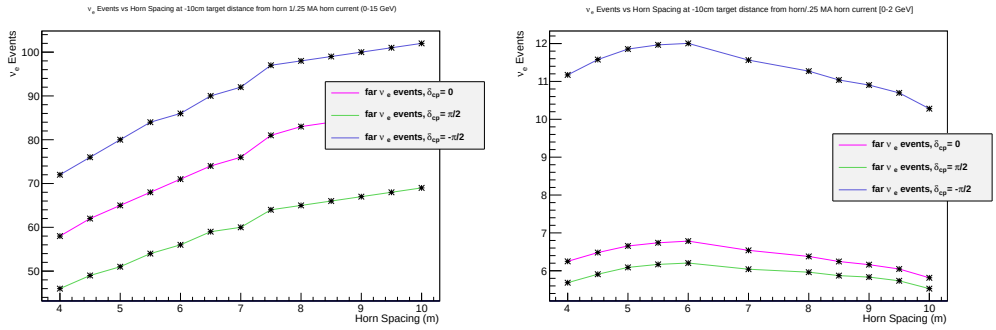

Figure 7: Neutrino events vs. Horn Spacing with target 10cm from horn 1 and .25 MA horn current over the 0-15 GeV and 0-2 GeV energy ranges, respectively.

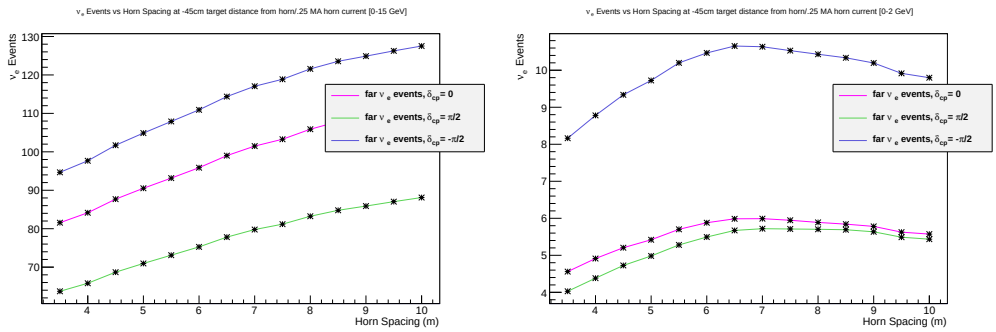

Figure 8: Neutrino events vs. Horn Spacing with target 45cm from horn 1 and .25 MA horn current over the 0-15 GeV and 0-2 GeV energy ranges, respectively. The same trend is seen when the target is and is not inserted.

From these plots, we see that for 0-15 GeV the optimal horn spacing is 10m which gives a 17.6% increase in electron neutrino yield over the current setup, and for 0-2 GeV the optimal horn spacing is 6m, which is currently what the beamline is setup for, therefore giving no increase in the yield. We also see that the same trend occurrs both when the target is and is not inserted in horn 1.

In determining the optimal configuration for horn current, target distance, and horn spacing, we see that for integration over the 0-15 GeV energy spectrum, the optimized geometry is 50cm target distance, 10m horn separation, and .30 MA in both horns. This complete optimization gives a total increase in electron neutrino flux yield of 56.7%. For integration over the 0-2 GeV energy range, the optimal solution is much different: 0cm target distance, 6m horn separation and .22 MA horn current. This 0-2 GeV optimization gives a total increase of 23.8%. This vast change in optimal geometry comes from the different requirements of focusing softer pions for the low energy range than simply just focusing as many pions as possible at whichever energy scale [4]. This difference can also be seen in the neutrino distribution histograms for both of the optimal cases when compared to one another:

From the plots shown in Figure 9, we see that the peak of the distribution is at a higher energy for the whole spectrum than the peak of the narrow 0-2 GeV energy spectrum. Additionally, we see that there are much different oscillatory properties of the muon neutrinos in the two different energy range

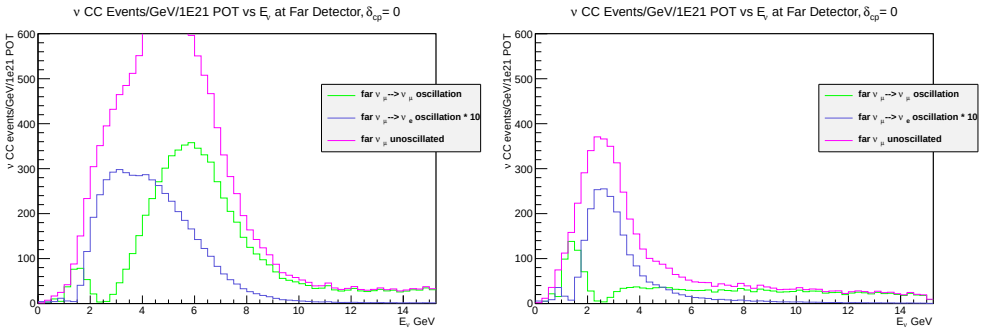

Figure 9: Neutrino Events vs. Neutrino Energy for the optimal cases over the 0-15 GeV spectrum (with 10m horn spacing) and 0-2 GeV, respectively.

optimal cases, as predicted by the probability curves in Figures 1 and 2. In addition to this, there is also a region where the two optimal regions overlap at 30-40cm target distance and .28-.30 MA horn current in both horns. As a measure of the approximate gain, at 30cm target distance and .28 MA (a point in this region)we see a gain in electron neutrino yiel of of 18.9% for 0-15 GeV and 14.9% for 0-2 GeV, both at 6m horn spacing. From this optimal intersection, the neutrino yield can be tuned by changing the horn spacing.

After finding the optimal target distance versus horn current and horn spacing, we held the target distance and horn spacing constant at 45cm and 6m, respectively, and varied the currents in horn 1 and horn 2. The plots in Figures 10 and 11 show electron neutrino events and the χ^2 fit vs horn 1 and 2 current.

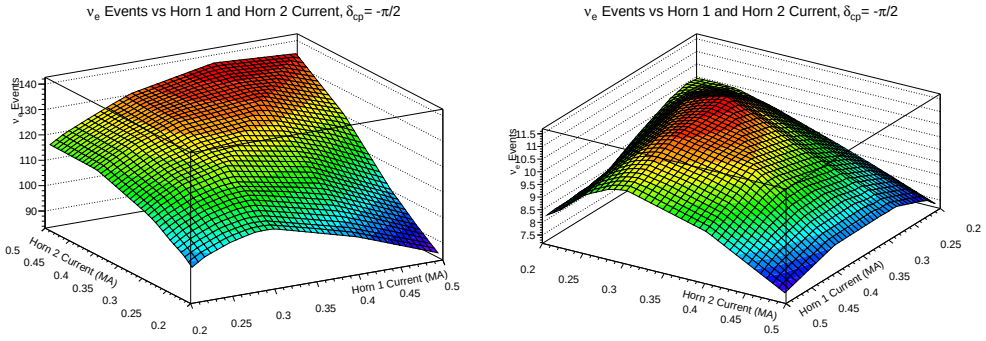

Figure 10: Electron Neutrino Events vs. horn 1 and horn 2 current over the 0-15 GeV spectrum and 0-2 GeV, respectively, with $\delta_{cp} = \pi/2$; target distance of 45cm and horn spacing at 6m.

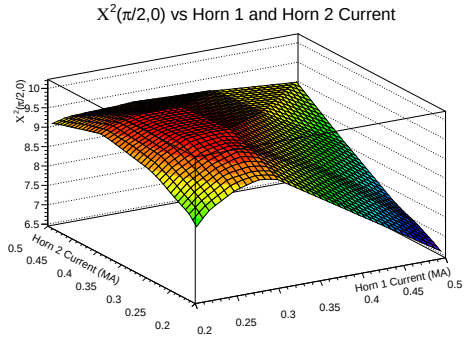

Figure 11: χ^2 fit comparing δ_{cp} =0, $\pi/2$ versus horn 1 and horn 2 current.

We see from the varied horn current plots that for 0-15 GeV the optimal horn currents are .40 MA for horn 1 and .50 MA for horn 2 and .30 MA and .30 MA. These optimizations give electron neutrino yield increases of 53.8% and 13.2% respectively. Additionally, we see a large area in the χ^2 plot where we have good sensitivity to δ_{cp}. Although these optimizations exist, they would be very difficult to implement not only due to the limitations of the horns themselves at very high current, but also because of the cost of separate power supplies for each horn. The 0-2 GeV optimization is within design feasibility, but the 0-15 GeV is far beyond the reach of current horn technology. A much more reasonable optimization is that of the target distance, current, and horn spacing.

5 Conclusion

We find that the most feasible solution is to optimize the horn current (keeping both the same), target distance, and horn spacing. The optimal arrangement for 0-15 GeV is 50cm target distance, 10m horn spacing, and .30 MA current in both horns. The optimal arrangement for 0-2 GeV is 0cm target distance, 6m horn spacing, and .22 MA current in both horns. These produce a electron neutrino yield increase of 56.7% and 23.8% when compared to the original LBNE beamline setup of 45cm target distance, 6m horn spacing, and .20 MA current in both horns. In short, we see a significant increase in events as compared to the current setup of the LBNE beamline with these changes. There is also an intersection of these two optimal regions around the range of 30-40cm target distance and .28-.30 MA at 6m horn separation, which give electron neutrino yield gains of 18.9% for 0-15 GeV and 14.9% for 0-2 GeV simultaneiously. Additionally, we see that these optimizations are the same independent of the CP angle, which makes these technical designs viable for any value of the parameter and thus simplifying the design possibilities. Modifying the existing horns so that the LBNE horn geometry matches these optimizations as closely as possible is an extremely cost-effective way to achieve drastic gains in neutrino production over the course of the experiment. Implementing these changes would certainly give the LBNE the best chance possible to discover the values of the CP angle δ_{cp} and the mass hierarchy of neutrinos and give physicists a much deeper understanding of the universe and our place in it [4].

References

[1] K. Nakamura et al. (Particle Data Group), "The Review of Particle Physics". J. Phys. G 37, 075021 (2010).

[2] R.N. Mohapatra *et. al.* "'The Theory of Neutrinos: A White Paper".Rept.Prog.Phys. **70** (2007) 1757. arXiv:hep-ph/0510213v2.

[3] P. Adamson *et al.* [MINOS Collaboration] "Search for the disappearance of muon antineutrinos in the NuMI neutrino beam." FERMILAB-PUB-11-357-PPD, BNL-96122-2011-JA, Phys.Rev.D84:071103,2011. arXiv:1108.1509

[4] T. Akiri *et al.* [LBNE Collaboration] "The 2010 Interim Report of the Long-Baseline Neutrino Experiment Collaboration Physics Working Groups" arXiv:1110.6249

[5] John R. Taylor "An Introduction to Error Analysis: The Study of Uncertainties in Physical Measurements." University Science Books (1982).

[6] S. Agostinelli *et. al.* "Geant4 - a simulation toolkit" Nucl. Inst. Meth. A 506, 250 (2003).

[7] J. Allison *et. al.* "Geant4 developments and applications." IEEE Transactions on Nuclear Science 53 No. 1, 270 (2006).

[8] Rene Brun and Fons Rademakers, "ROOT - An Object Oriented Data Analysis Framework", Proceedings AIHENP '96 Workshop, Lausanne, Sep. 1996, Nucl. Inst. and Meth. in Phys. Res. A 389 81 (1997).